HAMILTONIAN STABILITY OF SPIN–ORBIT RESONANCES IN CELESTIAL MECHANICS

ALESSANDRA CELLETTI[1] and LUIGI CHIERCHIA[2]
[1]*Dipartimento di Matematica, Università di Roma 'Tor Vergata', Via della Ricerca Scientifica, I–00133 Roma, Italy, e-mail: celletti@mat.uniroma2.it*
[2]*Dipartimento di Matematica, Università Roma Tre, Largo San Leonardo Murialdo 1, I–00146 Roma, Italy, e-mail: luigi@mat.uniroma3.it*

(Received: 15 June 1999; accepted: 17 July 2000)

Abstract. The behaviour of 'resonances' in the spin–orbit coupling in celestial mechanics is investigated in a conservative setting. We consider a Hamiltonian nearly-integrable model describing an approximation of the spin–orbit interaction. The continuous system is reduced to a mapping by integrating the equations of motion through a symplectic algorithm. We study numerically the stability of periodic orbits associated to the above mapping by looking at the eigenvalues of the matrix of the linearized map over the full cycle of the periodic orbit. In particular, the value of the trace of the matrix is related to the stability character of the periodic orbit. We denote by $\varepsilon_*(p/q)$ the value of the perturbing parameter at which a given elliptic periodic orbit with frequency p/q becomes unstable. A plot of the critical function $\varepsilon_*(p/q)$ versus the frequency at different orbital eccentricities shows significant peaks at the synchronous resonance (for low eccentricities) and at the synchronous and 3:2 resonances (at higher eccentricities) in good agreement with astronomical observations.

Key words: resonances, spin–orbit problem, periodic orbits, Hamiltonian dynamics

1. Introduction

This note is an attempt to justify from a purely conservative point of view why certain 'resonances' in the solar system are more common than others. By 'resonances' here we mean resonances in the spin–orbit problem, namely commensurabilities within the period of rotation and revolution of an oblate satellite orbiting around a central planet (see Goldreich and Peale, 1966, 1970; Peale, 1973; Murdock, 1978; Henrard, 1985; Wisdom, 1987; Celletti, 1990; Celletti and Falcolini, 1992; Celletti, 1994; Celletti and Chierchia, 1998, and references therein for related papers on this subject). As examples, we consider the Moon–Earth and Mercury–Sun systems. We then consider an extremely simple mathematical model for the spin–orbit problem, described by a time-periodic forced pendulum. In particular, we assume that an oblate satellite moves on a Keplerian orbit around a central planet and rotates about an internal spin-axis. We define a spin–orbit resonance of order $p : q$ whenever the ratio between the revolutional and rotational periods is rational, say $T_{\rm rev}/T_{\rm rot} = p/q$ for some positive integers p, q. The perturbing parameter is the equatorial oblateness of the satellite (the eccentricity of the

Celestial Mechanics and Dynamical Astronomy **76:** 229–240, 2000.

Keplerian orbit is considered as a given parameter). For a fixed frequency p/q, we compute the critical value $\varepsilon_*(p/q)$ at which the elliptic periodic orbit with frequency p/q becomes unstable, while it is stable for $0 < \varepsilon < \varepsilon_*(p/q)$. Such value is obtained by studying the trace of the linearized matrix over the full cycle of the periodic orbit. We then introduce the characteristic stability indicator $\sigma(p/q)$, which provides a measure of the stability of the different periodic orbits. The plot of $\sigma(p/q)$ vs. p/q shows that for low values of the eccentricity there is only a marked peak corresponding to the 1:1 commensurability (occurring when the periods of revolution and rotation are the same). Increasing the eccentricity, other resonances appear. Indeed, the 3:2 resonance can be observed at eccentricities larger than 0.01. Astronomical observations show that most of the evolved satellites or planets of the solar system are trapped in a 1:1 or 'synchronous' spin–orbit resonance. The most familiar example is provided by the Moon; due to the equality of the periods of rotation and revolution, the Moon always points the same face to the Earth. The only known exception is provided by Mercury, which moves in a 3:2 resonance.

The mathematical model for the spin–orbit motion (see Section 2) is described by an equation of the form

$$\ddot{x} - \varepsilon f_x(x, t) = 0, \tag{1.1}$$

for a suitable function f depending also on the orbital eccentricity e of the Keplerian orbit; the parameter ε is proportional to the equatorial oblateness coefficient of the satellite. The above equation can be rewritten as

$$\dot{x} = y, \qquad \dot{y} = \varepsilon f_x(x, t), \tag{1.2}$$

which can be viewed as Hamilton's equations associated to the non–autonomous, one-dimensional Hamiltonian

$$H(y, x, t) = \frac{y^2}{2} - \varepsilon f(x, t) ,$$

$y \in \mathbf{R}$, $x \in \mathbf{T} \equiv \mathbf{R}/2\pi\mathbf{Z}$ being conjugate coordinates and $t \in \mathbf{T}$. The variable x represents the angle between the longest axis of the ellipsoidal satellite and the periapsis line (see Figure 1) and $\dot{x} \equiv \mathrm{d}x/\mathrm{d}t$ represents its velocity.

In Section 3 we introduce a stability criterion for periodic orbits. Such criterion involves the computation of trajectories associated to periodic orbits. This is achieved by a method introduced by (Greene, 1979) for the standard map, which we generalize to our specific case in Appendix A. Results and conclusions are presented in Section 4.

2. The Spin–Orbit Model

We briefly recall a mathematical model introduced in (Celletti, 1990) to describe the 'spin–orbit' interaction in celestial mechanics. Let S be a triaxial ellipsoidal

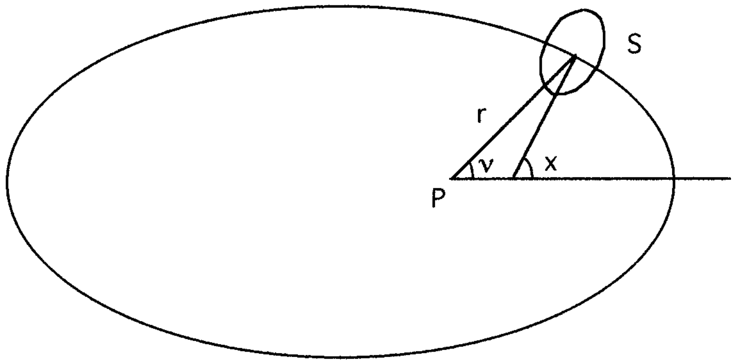

Figure 1. The spin-orbit geometry.

satellite orbiting around a central planet P. Let T_{rev} and T_{rot} be the periods of revolution of the satellite around P and the period of rotation about an internal spin-axis. A $p : q$ spin–orbit resonance occurs whenever

$$\frac{T_{\text{rev}}}{T_{\text{rot}}} = \frac{p}{q}\,, \quad \text{for } p, q \in \mathbf{N},\ q \neq 0.$$

In particular, when $p = q = 1$ we speak of 1:1 or synchronous spin–orbit resonance, which implies that the satellite always points the same face towards the host planet. In the solar system most of the evolved satellites or planets (e.g., the Moon) are trapped in a 1:1 resonance (Astronomical Almanac, 1997). The only exception is provided by Mercury which is observed in a nearly 3:2 resonance.

We introduce a mathematical model describing the spin–orbit interaction. In particular we assume that:

(i) the center of mass of the satellite moves on a Keplerian orbit around P with semimajor axis a and eccentricity e;
(ii) the spin-axis is perpendicular to the orbit plane;
(iii) the spin-axis coincides with the shortest physical axis (i.e., the axis whose moment of inertia is largest);
(iv) dissipative effects as well as perturbations due to other planets or satellites are neglected.

Remark. Assumptions (i) and (ii) imply that we neglect secular perturbations on the orbital parameters as well as the obliquity of the spin–axis. As shown in (Laskar and Robutel, 1993) a more relevant model from the physical point of view needs to consider a non-Keplerian orbit as well as a non-zero obliquity. However, our model may be considered as a starting point to study the spin–orbit dynamics at the most elementary level. Results could be generalized so as to include secular perturbations and the spin–axis obliquity. In particular, as is well known in the case of the Mercury–Sun system it is definitely important to include the effect of secular variations of the elliptic elements.

We introduce now a mathematical model (compare with Celletti, 1990) apt to describe the spin–orbit interaction under the above assumptions. Let $A < B < C$ be the principal moments of inertia of the satellite. We denote by r and ν, respectively, the instantaneous orbital radius and the true anomaly of the Keplerian orbit. Finally, let x be the angle between the longest axis of the ellipsoid and the periapsis line (see Figure 1). The equation of motion may be derived from the standard Euler's equations for rigid body. In normalized units (i.e. assuming that the mean motion is one, $2\pi/T_{\rm rev} = 1$) we obtain

$$\ddot{x} + \varepsilon \left(\frac{1}{r}\right)^3 \sin(2x - 2\nu) = 0 , \tag{2.1}$$

where $\varepsilon \equiv 3/2(B - A)/C$ is proportional to the equatorial oblateness coefficient $(B - A)/C$ (and the dot denotes time differentiation). Notice that (2.1) is trivially integrated when $A = B$ or in the case of zero orbital eccentricity.

Due to assumption (i), the quantities r and ν are known (periodic) Keplerian functions of the time; therefore we can expand (2.1) in Fourier series as

$$\ddot{x} + \varepsilon \sum_{m\neq 0, m=-\infty}^{\infty} W\left(\frac{m}{2}, e\right) \sin(2x - mt) = 0 , \tag{2.2}$$

where the coefficients $W(m/2, e)$ decay as powers of the orbital eccentricity as $W(m/2, e) \propto e^{|m-2|}$ (see Cayley 1859, for explicit expressions).

A further simplification of the model is performed as follows. According to assumption (iv), we neglected dissipative forces and any gravitational attraction beside that of the central planet. The most important contribution comes from the non-rigidity of the satellite, which provokes a tidal torque due to internal friction. Since the magnitude of the dissipative effects is small compared to the gravitational term, we simplify (2.2) retaining only those terms which are of the same order or bigger than the average effect of the tidal torque. Thus we are led to consider an equation of the form

$$\ddot{x} + \varepsilon \sum_{m\neq 0, m=N_1}^{N_2} \tilde{W}\left(\frac{m}{2}, e\right) \sin(2x - mt) = 0 , \tag{2.3}$$

where N_1 and N_2 are suitable integers (depending on the structural and orbital properties of the satellite), while $\tilde{W}(m/2, e)$ are truncations of the coefficients $W(m/2, e)$ (which are power series in e).

In this paper we are mainly concerned with the Moon–Earth and the Mercury–Sun systems. In the case of the Moon–Earth system N_1 and N_2 are, respectively, 1 and 7. For such system we obtain the equation

$$\ddot{x} + \varepsilon \Bigg[\left(-\frac{e}{2} + \frac{e^3}{16} \right) \sin(2x - t) + + \left(1 - \frac{5}{2}e^2 + \frac{13}{16}e^4 \right) \sin(2x - 2t) + \left(\frac{7}{2}e - \frac{123}{16}e^3 \right) \sin(2x - 3t) + + \left(\frac{17}{2}e^2 - \frac{115}{6}e^4 \right) \sin(2x - 4t) + \left(\frac{845}{48}e^3 - \frac{32525}{768}e^5 \right) \sin(2x - 5t) + + \frac{533}{16}e^4 \sin(2x - 6t) + \frac{228347}{3840} e^5 \sin(2x - 7t) \Bigg] = 0. \tag{2.4}$$

Notice that the largest coefficient (of order unity) corresponds to the synchronous resonance (i.e., the term related to $2x - 2t$). For $e = 0$ Equation (2.4) reduces to $\ddot{x} + \varepsilon \sin(2x - 2t) = 0$ which corresponds to a pendulum (after the substitution $x \to x - t$). Other examples, such as the Mercury–Sun system, would be described by a different Fourier series truncation (for the Mercury–Sun case, it is $N_1 = -17$, $N_2 = 6$ in (2.3) and with slightly different truncations of the $\tilde{W}$'s); however, we checked that results do not change significantly as new terms are added to Equation (2.4). Precisely, more terms alter the outputs for any initial condition, provoking a global rescaling of the results, without conditioning the qualitative conclusions. The (non-integrable) dynamics of (2.4) is represented in Figure 2 by the Poincaré (or stroboscopic) map (at $t = 2\pi$) around the synchronous resonance

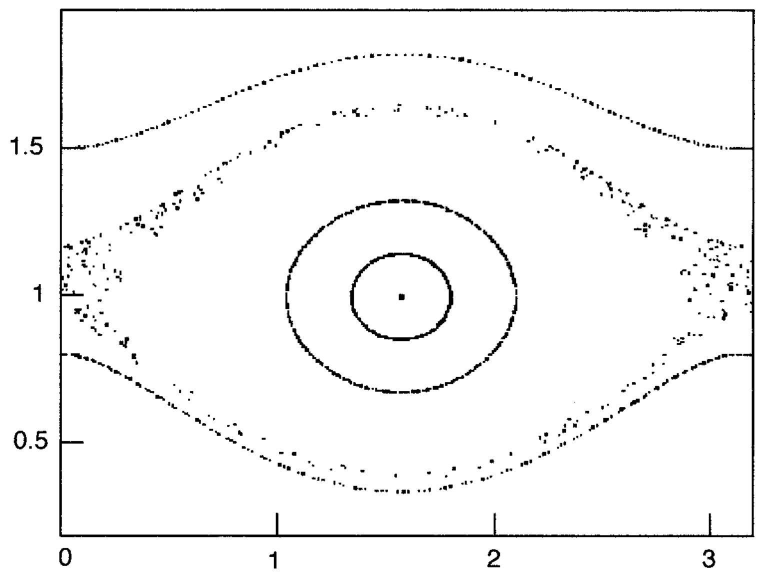

Figure 2. Poincaré map associated to Equation (2.4) around the synchronous resonance in the $(x, \dot{x})$–plane for $e = 0.004$, $\varepsilon = 0.2$. The initial conditions are $(x, y) = (0, 0.8)$, $(0, 1.5)$, $(0, 1)$, $(0, 1.1)$, $(1.8, 1)$, $(2.1, 1)$, $(1.57, 1)$. Notice that Equation (2.4) is π–periodic in x. Librational and rotational regions are divided by the chaotic separatrix.

for $e = 0.004$, $\varepsilon = 0.2$: the resonance is surrounded by librational surfaces, whose amplitude increases as the chaotic separatrix is approached. Outside this region rotational surfaces can be found.

3. Stability Criterion For Periodic Orbits

In this section we investigate numerically the stability of the periodic orbits. We define a '$p : q$ periodic orbit' (or Birkhoff periodic orbit with rotation number p/q) as a solution of (1.1), $x : \mathbf{R} \to \mathbf{R}$, such that

$$x(t + 2\pi q) \ = \ x(t) + 2\pi p, \tag{3.1}$$

that is, after q orbital revolutions around the central body the satellite makes p rotations about the spin-axis.

By applying a symplectic Euler's method with step size h to the differential equations (1.2), we are led to study the mapping

$$y_{n+1} = y_n + \varepsilon f_x(x_n, t_n)\, h, \qquad x_{n+1} = x_n + y_{n+1} h, \qquad t_{n+1} = t_n + h. \tag{3.2}$$

Notice that the determinant of the jacobian of the mapping (3.2) is identically one. Let M be the product of the jacobian of (3.2) over the full cycle of the periodic orbit with frequency p/q, that is,

$$M = \prod_{i=1}^{q} \begin{pmatrix} 1 & \varepsilon f_{xx}(x_i, t_i) h \\ h & 1 + \varepsilon f_{xx}(x_i, t_i) h^2 \end{pmatrix},$$

where the points (x_i, t_i), $i = 1, \ldots, q$, are computed along the periodic orbit. Following (Greene, 1979) the three-dimensional search (in the variables y, x, t) for periodic orbits can be reduced to a one-dimensional problem, using the symmetry property of the mapping (3.2). In particular, use is made of the fact that the mapping (3.2) can be decomposed as the product of two involutions. The initial value of a periodic orbit can be found along the lines of fixed points of one of the above involutions. More details about this method can be found in Appendix A (see also Celletti, 1990). The eigenvalues of M are the associated Floquet multipliers; due to the area–preserving property of (3.2), one has $\det M = 1$. Therefore, the product of the eigenvalues λ_1, λ_2 of M is unity, while their sum equals the trace T of M: $\lambda_1 + \lambda_2 = T$. Since λ_1, λ_2 must satisfy the equation $\lambda^2 - T\lambda + 1 = 0$, one finds

$$\lambda_{1,2} = \frac{T}{2} \pm i\sqrt{1 - \left(\frac{T}{2}\right)^2}.$$

According to the value of T, one has different solutions for the eigenvalues providing the stability character of the periodic orbit as follows:

(i) if $|T| < 2$, then λ_1, λ_2 are complex conjugates on the unit circle and the motion is stable;
(ii) if $|T| > 2$, λ_1 and λ_2 are real numbers with $\lambda_2 = \lambda_1^{-1}$ and one of the eigenvalues is in modulus greater than 1, providing the instability of the periodic orbit.

Notice that in the integrable case $\varepsilon = 0$, $T = 2$ and $\lambda_{1,2} = 1$. As is well known, for any value of the frequency p/q there exist, in general, periodic orbits of elliptic *and* hyperbolic type. We are interested in investigating the stability of the elliptic periodic orbits as the perturbing parameter ε is increased. In particular, for a fixed eccentricity we look at the value of ε at which the trace T, which originates from the value $T = 2$ as $\varepsilon = 0$, decreases down to the transition value $T = -2$ becoming, immediately after, $T < -2$. We denote by $\varepsilon_*(p/q)$ the value of the perturbing parameter at which the transition occurs. We take the behaviour of $\varepsilon_*(p/q)$ versus the frequency $\frac{p}{q}$ as an index of stability. The graph of the analog of the critical function $\varepsilon_*(\omega)$ versus ω (diophantine) for invariant tori (i.e. the so-called 'breakdown threshold') of the spin-orbit problem has been investigated in (Celletti and Falcolini, 1992).

Next, we want to give a *weight* to peaks of the function ε_*; this weight should take into account, besides the absolute magnitude of the peak, also its *relative* value compared to nearby (eventually smaller) peaks, or its degree of isolation (an isolated peak is 'more stable' than a peak with other closeby peaks of comparable magnitude), etc. We proceed as follows: assume that ε_* has a peak (a relative maximum) at $\omega_0 = p/q$; let δ_0 be a positive real number such that $\varepsilon_*(\omega_0+\delta_0) = \varepsilon_*(\omega_0)$ or $\varepsilon_*(\omega_0-\delta_0) = \varepsilon_*(\omega_0)$, and $\varepsilon_*(\omega') < \varepsilon_*(\omega_0)$ for any $\omega' \in I_0(\delta_0) \equiv (\omega_0-\delta_0, \omega_0+\delta_0)\backslash\{\omega_0\}$. Then, the quantity

$$\alpha(\omega_0, \delta_0) \equiv \max_{\omega' \in I_0(\delta_0)} \frac{\varepsilon_*(\omega_0) - \varepsilon_*(\omega')}{\varepsilon_*(\omega_0)|\omega_0 - \omega'|}$$

provides the relative distance of the transition values in a neighbourhood of size δ_0 around the frequency ω_0. In order to have an indicator of stability, we multiply $\alpha(\omega_0, \delta_0)$ by the half size of the domain $I_0(\delta_0)$, that is we define the characteristic stability indicator (hereafter, CSI) as $\sigma(\omega_0) \equiv \delta_0\, \alpha(\omega_0, \delta_0)$. We will see in the next section that the plot of $\sigma(\omega_0)$ versus ω_0 provides useful informations about stability properties of periodic orbits.

4. Results and Conclusions

According to standard evolutionary theories, satellites and planets were rotating fast in the past; a constant decrease of the period of rotation about the spin-axis was provoked by tidal friction due to the internal non-rigidity. Therefore, a common scenario suggests that celestial bodies were slowed down until they reached their actual dynamical configuration, being typically trapped in a 1:1 (with the 3:2 Mercury exception) resonance. This hypothesis implies that higher order resonances (i.e., 2:1, 5:4, 7:3, etc.) were bypassed during the slowing process. Beside the tidal effect, a parameter which might direct the motion toward a resonance is the orbital eccentricity.

In this section we investigate the stability of the resonant motions corresponding to periodic orbits as the orbital eccentricity is varied. More precisely, we compute the critical value $\varepsilon_*(p/q)$ and the CSI $\sigma(p/q)$ for different periodic orbits of frequency p/q. We let the eccentricity vary in a reasonable (astronomical) range of values. In particular, we consider the following set of periodic orbits with frequencies p/q where

$$q = 1, \dots, 14, \qquad p = q + 1, \dots, 15,$$

and

$$p = 1, \dots, 14, \qquad q = p + 1, \dots, 15.$$

In order to have a better precision around the main resonances we consider also the periodic orbits with frequencies

$$\begin{array}{ll} \frac{1}{2} \pm \frac{1}{10 \cdot k}, & 1 \pm \frac{1}{10 \cdot k}, \\ \frac{5}{4} \pm \frac{1}{10 \cdot k}, & \frac{4}{3} \pm \frac{1}{10 \cdot k}, \\ \frac{3}{2} \pm \frac{1}{10 \cdot k}, & \frac{5}{3} \pm \frac{1}{10 \cdot k}, \\ \frac{7}{4} \pm \frac{1}{10 \cdot k}, & 2 \pm \frac{1}{10 \cdot k}, \end{array}$$

where $k = 1, \dots, 10$.

For a fixed value of the eccentricity we compute $\varepsilon_*(p/q)$ and $\sigma(p/q)$ corresponding to the set of rational numbers p/q listed above. Figures 3 and 4 show the graphs of $\varepsilon_*(p/q)$ and $\sigma(p/q)$ versus p/q for, respectively, the Moon's eccentricity (i.e., $e = 0.0549$) and Mercury's eccentricity ($e = 0.2056$). In order to have a better understanding of the behaviour around the resonances of astronomical interest, we report in panel (a) the results around the 1:2 resonance, while panel (b) corresponds to the synchronous resonance, panel (c) to the 3:2 resonance and panel (d) to the 2:1 resonance.

A comparison between the graphs of $\sigma(p/q)$ vs. p/q reported in Figures 3 and 4 indicates that the most stable resonances are the 1:1, 3:2 and 2:1. However, the stability indicator changes as the eccentricity is varied. In particular, the 1:1 resonance is the most stable one for the Moon's eccentricity (see Figure 3). When the eccentricity is increased up to Mercury's value (i.e. $e = 0.2056$), the 3:2 resonance gains stability and its CSI becomes comparable to that of the synchronous

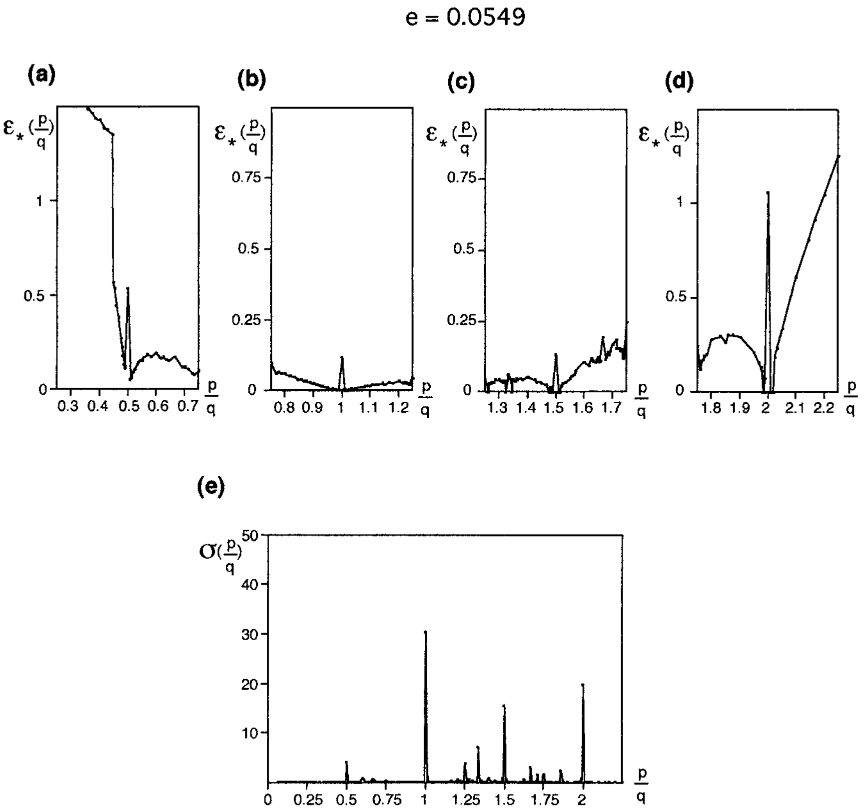

Figure 3. The transition value $\varepsilon_*(p/q)$ vs. p/q for $e = 0.0549$ (i.e. the eccentricity of the Moon). The dots correspond to the actual computations associated to the frequencies listed in the text. Lines are due to interpolation performed by the graphic program. In abscissa are reported the rotation numbers p/q (the 1:1 resonance corresponds to 1, the 1:2 to 0.5 and so on). (a) 1:2 resonance, (b) 1:1 resonance, (c) 3:2 resonance, (d) 2:1 resonance. (e) The CSI $\sigma(p/q)$ vs. p/q for $e = 0.0549$.

resonance (see Figure 4). This remark suggests that the higher value of the eccentricity might be responsible of the actual dynamical configuration of Mercury in the 3:2 resonance. Indeed, it is worth noticing that the 1:1 and 3:2 resonances attain a comparable stability level for a value of the eccentricity of the order of $e = 0.2$. At lower values of e, for example $e = 0.1$ as in Figure 5(c), the motion associated to the synchronous resonance is still the most stable one. We report in Figure 5 the behaviour of $\varepsilon_*(p/q)$ and of $\sigma(p/q)$ for $e = 0.001$ (Figure 5(a)), $e = 0.01$ (Figure 5(b)), $e = 0.1$ (Figure 5(c)). A comparison among the different graphs suggests that resonances different from the synchronous one are born as the eccentricity is increased, while at low values of the eccentricity, say $e = 0.001$, the 1:1 resonance is rather isolated. This result is supported by the astronomical observations, since most of the satellites observed to move in the synchronous resonance have eccentricities in the range [0, 0.01] (see Astronomical Almanac, 1997).

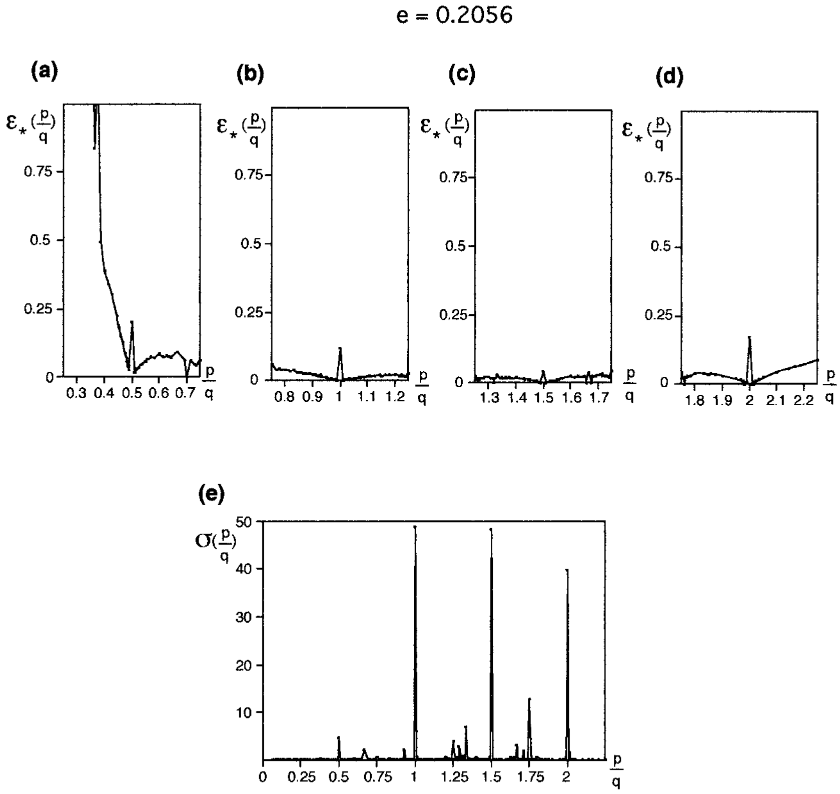

Figure 4. The transition value $\varepsilon_*(p/q)$ vs. p/q for $e = 0.2056$ (i.e., the eccentricity of Mercury). The dots correspond to the actual computations associated to the frequencies listed in the text. Lines are due to interpolation performed by the graphic program. In abscissa are reported the rotation numbers p/q (the 1:1 resonance corresponds to 1, the 1:2 to 0.5 and so on). (a) 1:2 resonance, (b) 1:1 resonance, (c) 3:2 resonance, (d) 2:1 resonance. (e) The CSI $\sigma(p/q)$ vs. p/q for $e = 0.2056$.

We finally mention that for a further development of this study it would be clearly necessary to include the spin-axis obliquity as well as the effect of dissipative terms. In the latter case one is led to the question of the existence of attracting tori for a dissipative system (i.e., including tidal forces) corresponding to the most stable resonances. We plan to address this problem in a later study.

Appendix A: Computation of Periodic Orbits

Let S be the mapping (3.2) which we rewrite as

$$y' = y + \varepsilon f_x(x, t)\, h, \qquad x' = x + y'\, h, \qquad t' = t + h,$$

where $y, x, t \in \mathbf{R}$. Finding periodic orbits associated to S can be considerably simplified exploiting the symmetry property of S. Indeed, this fact was already observed in (Greene, 1979) for the standard mapping

$$y' = y + \varepsilon \sin x, \qquad x' = x + y'.$$

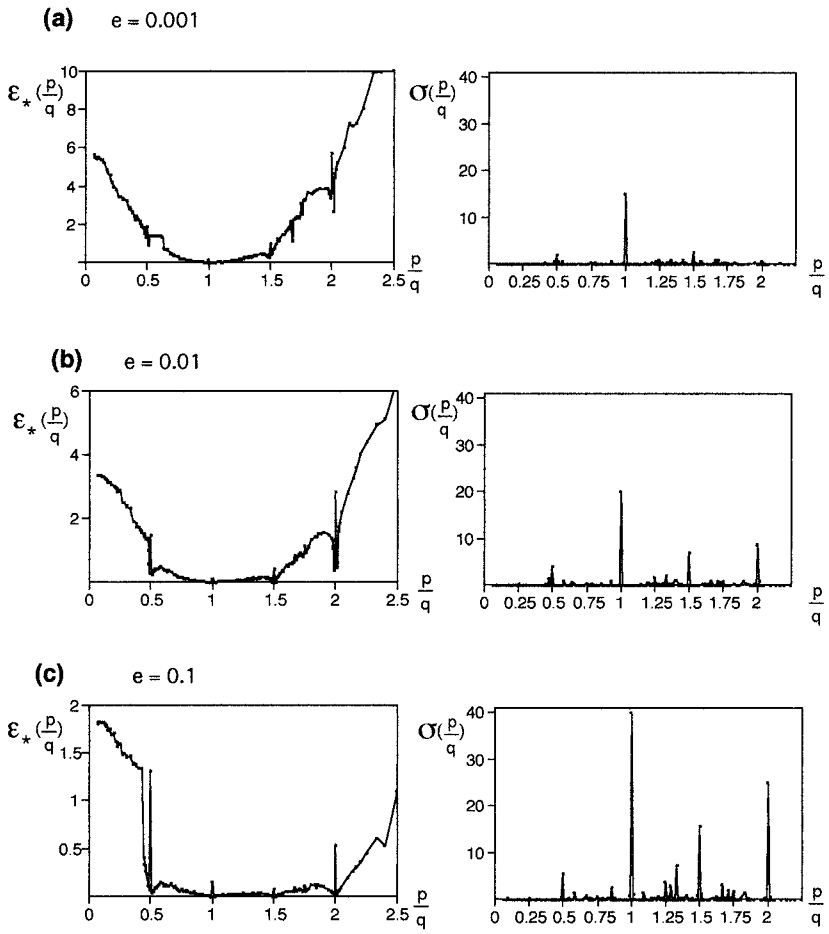

Figure 5. Left panel: plot of $\varepsilon_*(p/q)$ vs. p/q for the frequencies listed in the text; right panel: plot of the CSI $\sigma(p/q)$ vs. p/q for the same frequencies as in the left panel. (a) $e = 0.001$, (b) $e = 0.01$, (c) $e = 0.1$.

($y \in \mathbf{R}$, $x \in \mathbf{R}/2\pi\mathbf{Z}$) and can be generalized to our case as follows. The basic remark is that S can be decomposed as the product of two involutions:

$$S = I_2\, I_1\ , \qquad I_1^2 = I_2^2 = 1\ , \qquad I_2 = SI_1,$$

where I_1 is given by

$$y' = y + \varepsilon f_x(x,t)h, \qquad x' = -x, \qquad t' = -t,$$

and I_2 is defined as

$$y' = y, \qquad x' = -x + h\, y, \qquad t' = -t + h.$$

The periodic orbits correspond to fixed points of I_1 or I_2 (Greene, 1979, Appendix A). Since the function $f_x(x,t)$ is π-periodic in x and 2π periodic in the time, the periodic orbits can be found at $(x, t) = (0, 0)$, $(\pi/2, 0)$, $(0, \pi)$, $(\pi/2, \pi)$. This reduces the search for periodic orbits to a one-dimensional problem in the y variable.

References

Cayley, A.: 1859, ‘Tables of the developments of functions in the theory of elliptic motion’, *Mem. Roy. Astron. Soc.* **29**, 191.

Celletti, A.: 1990, ‘Analysis of resonances in the spin-orbit problem in celestial mechanics: The synchronous resonance’, (*Part I*) *J. Appl. Math. Phys. (ZAMP)* **41**, 174; *Part II: ZAMP* **41**, 453.

Celletti, A.: 1994, ‘Construction of librational invariant tori in the spin-orbit problem’, *J. Applied Math. Physics (ZAMP)* **45**, 61.

Celletti, A. and Chierchia, L.: 1998, ‘Construction of stable periodic orbits for the spin-orbit problem of celestial mechanics’, *Reg. Chaotic Dyn.* **3**, 107.

Celletti, A. and Falcolini, C.: 1992, ‘Construction of invariant tori for the spin-orbit problem in the Mercury–Sun system’, *Celest. Mech. & Dyn. Astr.* **53**, 113.

Greene, J. M.: 1979, ‘A method for determining a stochastic transition’, *J. Math. Phys.* **20**, 1183.

Goldreich, P. and Peale, S.: 1966, ‘Spin–orbit coupling in the solar system’, *Astron J.* **71**, 425.

Goldreich, P. and Peale, S.: 1970, ‘The dynamics of planetary rotations’, *Ann. Rev. Astron. Astroph.* **6**, 287.

Henrard, J.: ‘Spin-orbit resonance and the adiabatic invariant’, in: S. Ferraz–Mello and W. Sessin (eds), *Resonances in the Motion of Planets, Satellites and Asteroids*, Sao Paulo, 19.

Laskar, J., Robutel, P.: 1993, ‘The chaotic obliquity of the planets’, *Nature* **361**, 608.

Murdock, J. A.: 1978, ‘Some mathematical aspects of spin-orbit resonance I’, *Celest. Mech. & Dyn. Astr.* **18**, 237.

Peale, S. J.: 1973, ‘Rotation of solid bodies in the solar system’, *Rev. Geoph. Space Phys.* **11**, 767.

Wisdom, J.: 1987, ‘Rotational dynamics of irregularly shaped satellites’, *Astron. J.* **94**, 1350.

(No author listed) 1997, *The Astronomical Almanac*. Washington: U.S. Government Printing Office.